Final Analysis and Results of the Phase II SIMPLE Dark Matter Search

M. Felizardo,[1,2] T. A. Girard,[2,*] T. Morlat,[3] A. C. Fernandes,[4,2] A. R. Ramos,[4,2] J. G. Marques,[4,2] A. Kling,[4,2] J. Puibasset,[5]
M. Auguste,[6] D. Boyer,[6] A. Cavaillou,[6] J. Poupeney,[6] C. Sudre,[6] H. S. Miley,[7] R. F. Payne,[7] F. P. Carvalho,[4]
M. I. Prudêncio,[4] A. Gouveia,[4] and R. Marques[4]

(The SIMPLE Collaboration)

[1]*Department of Physics, Universidade Nova de Lisboa, 2829-516 Caparica, Portugal*
[2]*Centro de Física Nuclear, Universidade de Lisboa, 1649–003 Lisbon, Portugal*
[3]*Ecole Normale Superieur de Montrouge, 1 Rue Aurice Arnoux, 92120 Montrouge, France*
[4]*Instituto Tecnológico e Nuclear, Instituto Superior Técnico, Universidade Técnica de Lisboa, EN 10, 2686-953 Sacavém, Portugal*
[5]*CRMD-CNRS and Université d'Orléans, 1 bis Rue de la Férollerie, 45071 Orléans, France*
[6]*Laboratoire Souterrain de Rustrel Pays d'Apt, UMS 3538 UNS/UAPV/CNRS, 84400 Rustrel, France*
[7]*Pacific Northwest National Laboratory, Richland, Washington 99352, USA*
(Received 15 June 2011; revised manuscript received 15 March 2012; published 18 May 2012)

We report the final results of the Phase II SIMPLE measurements, comprising two run stages of 15 superheated droplet detectors each, with the second stage including an improved neutron shielding. The analyses include a refined signal analysis, and revised nucleation efficiency based on a reanalysis of previously reported monochromatic neutron irradiations. The combined results yield a contour minimum of $\sigma_p = 5.7 \times 10^{-3}$ pb at 35 GeV/c^2 in the spin-dependent sector of weakly interacting massive particle (WIMP) proton interactions, the most restrictive to date for $M_W \leq 60$ GeV/c^2 from a direct search experiment and overlapping, for the first time, with results previously obtained only indirectly. In the spin-independent sector, a minimum of 4.7×10^{-6} pb at 35 GeV/c^2 is achieved, with the exclusion contour challenging a significant part of the light mass WIMP region of current interest.

The search for weakly interacting massive particle (WIMP) dark matter remains at the forefront of modern physics activity. Estimated to comprise ~23% of the Universe mass, it is the role of direct detection efforts to elaborate its nature, and whether its interaction with nucleons is spin-independent (SI) or spin-dependent (SD). Superheated Instrument for Massive ParticLe Experiments (SIMPLE) [1] is a direct search activity using superheated liquid detectors, and one of only a few in the international panorama with sensitivity to the WIMP-proton sector of the SD phase space. It is operated at the 1500 mwe level of the Low Noise Underground Laboratory (LSBB) in southern France.

In [1], we reported the first results of a two stage Phase II measurement, comprising a 14.1 kgd Stage 1 exposure of 15 superheated droplet detectors (SDDs) [2–4] with a total active mass of 0.208 kg. We here provide the results of the full Phase II measurement, including a 13.67 kgd Stage 2 exposure of a second 15 SDD set, together with improved neutron shielding and a refined analysis of the individual detector run signals, sensitivities, and nucleation efficiency.

A SDD consists of a dispersion of superheated liquid droplets homogeneously distributed within a gel matrix, which may undergo a transition to the gas phase upon energy deposition by incident radiation. Two conditions are required for the nucleation of the gas phase of the superheated droplets [5]: (i) the energy deposited must be greater than a thermodynamic minimum, and (ii) this energy must be deposited within a thermodynamically defined minimum distance (Λr_c) inside the droplet, where Λ is the nucleation parameter and r_c equals the thermodynamic critical bubble radius. Adjustment of the two conditions results in the necessity of depositions of order $\geq$ 150 keV/μm for a bubble nucleation, rendering the SDD effectively insensitive to the majority of traditional detector backgrounds (including electrons, γ's, and cosmic muons) which complicate more conventional dark matter search detectors, leaving only α- and neutron-induced events.

The 15 Stage 2 SDDs were fabricated as described in [1], each containing between 11–19 g of C_2ClF_5 for a total active mass of 0.215 kg; an additional, freonless, but otherwise identical, SDD again served as an acoustic veto. These were initially pressurized to 2.00 ± 0.05 bar, and installed at the rate of one per day in a 700 l water pool maintained at a bath temperature of $9.0 \pm 0.1\,°C$, this time with the data acquisition initiated only after the installation of each 8 detector set. The instrumentation was identical to that of Stage 1; in contrast to Stage 1, however, the SDD pressures were allowed to rise with time in order to obtain additional information on the measurement sensitivity.

Also, in contrast to Stage 1, the water pool rested on an additional 10 cm of wood and paraffin, and 10 cm of

polyethylene, with a rebuilt 50–75 cm thick surrounding water shield. As a result of the seasonal increase in water circulation within the mountain, the ambient radon level increased to $\sim$1000 Bq/m^3; continued purging of the cavern air reduced this to $\sim$100 Bq/m^3, and circulation of the pool water in combination with radioassays of the detector construction materials yielded a Stage 2 α-background estimate, including both progenitor and daughter decays, of 5.72 ± 0.12(stat) ± 0.29(syst) evt/kgd.

Extensive Monte Carlo estimates of the expected neutron background, which accounted for spontaneous fission plus decay-induced (α, n) reactions, and included the increased below-pool shielding and new materials radioassays, yielded a reduced rate of 0.333 ± 0.001(stat) ± 0.038(syst) evt/kgd; recalculation of the Stage 1 disposition with the new radioassays yielded a revised background rate of 0.976 ± 0.004(stat) ± 0.042(syst) evt/kgd, with the primary contribution being the concrete. For the improved shielding of Stage 2, background neutrons originate mainly from the glass detector containment and shield water.

Stage 2 data were obtained between 12 April–22 July 2010. The total exposure was 13.67 kgd, from the detector installation protocol and mechanical failure of 4 SDDs during the run as a result of overpressuring; no weather-induced data losses occurred.

The analysis of the Stage 2 signals, as per Stage 1, included a filtering of the initial data set (1997 events) via a pulse validation routine, a cross correlation of the remaining set in time between all SDDs, and coincidence rejection as due to local noise events and that a WIMP interacts with no more than one of the in-bath detectors [1]; the analysis was improved via a new bandpass filter for noise suppression. The signal waveform, decay time constant, and spectral density structure of the remaining 826 single events were next inspected individually. A particle-induced nucleation event possesses a characteristic frequency response, with a time span of a few milliseconds, a decay constant of 5–40 ms, and a primary harmonic between 0.45–0.75 kHz; these parameters differ significantly from those of gel-associated acoustic backgrounds such as trapped N$_2$ gas, fractures, and local acoustic backgrounds such as water bubbles [6]. The event-by-event analysis permits isolation of the particle-induced nucleation events with an efficiency of better than 97% at 95% C.L.

Figure 1 displays the signal amplitude and frequency for each of the identified 41 particle-induced signal events in Stage 2. Following calibrations as described in [1], a nuclear recoil discrimination cut for $A \leq 100$ mV was again imposed with an acceptance of $>$97%, yielding a total of 2 events for the entire exposure.

The two bubble nucleation criteria are thermodynamic [5], so that variation of either temperature or pressure modifies the recoil threshold energy and thus the SDD
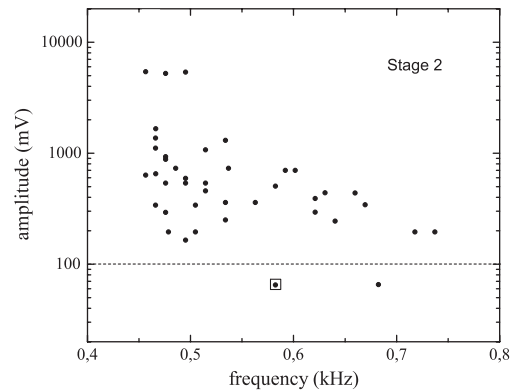

FIG. 1. Scatter plot of the amplitudes and frequency of the primary harmonic of each true nucleation event observed over the Stage 2 exposure, with the boxed event for pressures ≤ 2.2 bar.

sensitivity, as seen in Fig. 2 where the expected variation in threshold recoil energies (E_{thr}) of both neutron-induced recoils and α's for several operating pressures is shown. The α threshold curve shifts to higher temperatures with increasing pressure. Since the curves depend on Λ [5], a comparison of experiment and theoretical predictions with varying Λ confirmed our measurements [7] of $\Lambda = 1.40 \pm 0.05$, yielding no α sensitivity whatsoever above 2.30 bar as observed experimentally. This was then used in calculating the ion recoil energy curves shown in Fig. 2. For pressures $\leq 2.20 \pm 0.05$ bar, the threshold recoil energy at 9 °C remains below 9.0 ± 0.3 keV.

As also seen in Fig. 2, the ion recoil threshold curves similarly evolve to higher temperatures and energies with pressure increase, rendering the SDDs increasingly less responsive to the on-detector neutron spectrum: at 2.50 bar, this reduction is 30%, which is consistent with
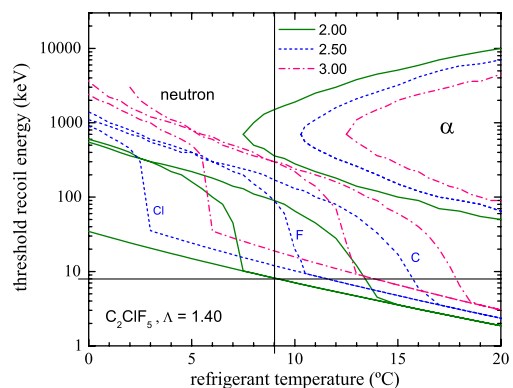

FIG. 2 (color online). Variation of the recoil and α energy thresholds with temperature for the three C$_2$ClF$_5$ constituents at 2.00 (solid lines), 2.50 (dashed lines), and 3.00 (dash-dotted line) bar, with $\Lambda = 1.40$. The freon constituents are identified for 2.5 bar. The vertical line indicates the 9 °C measurement temperature; the horizontal line, a threshold recoil energy of 8 keV.

the observed absence of any low amplitude events above 2.3 bar when weighted by the exposure.

The pressure records of all SDDs were next inspected for evolution during the measurement, and correlated with the signal records. Data obtained at pressures greater than 2.20 bar were excluded, reducing the Stage 2 exposure to 6.71 kgd; correlation with the signal record yielded 1 recoil event consistent with the estimated 2.2 ± 0.3 background neutrons. The Stage 1 events were similarly pressure correlated, reducing the exposure to 13.47 kgd; reanalysis of the recoil signals via a Hilbert transform-based demodulation identified four events with exponential decay characteristic of nonuniform impulses observed in acoustic background studies associated with SDDs in vibrational contact with their support and air bubbles from water inflow, reducing the recoil events to 10, which is slightly below the estimated 13 ± 0.6 background neutrons.

The first Stage 1 results resulted in part from a theoretical bubble nucleation efficiency given by $\eta(E) = 1 - E_{\text{thr}}/E_{\text{dep}}$ [8]. This η, however, represents only a first approximation to the statistical nature of the energy deposition and its conversion into heat [9]: a detailed reanalysis of previous monochromatic (54 and 149 keV) neutron irradiation data [10], at 1 and 2 bar as a function of temperature, yielded a refined efficiency of $\eta' = 1 - \exp[-\Gamma(E/E_{\text{thr}} - 1)]$ with $\Gamma = 4.2 \pm 0.3$, independent of pressure.

We show in Fig. 3 the impacts of the Stage 2 and reanalyzed Stage 1 results on SD WIMP-proton scattering, together with the competitive results of other direct [11–13] and indirect [14,15] experiments. The contours are calculated using the previous [1] Feldman-Cousins approach [16] based on observing n events against a back-ground one systematic uncertainty below the estimated neutron-generated recoil background, η' with $\Gamma = 3.6$, the standard isothermal halo and a WIMP scattering rate [17] with zero momentum transfer, spin-dependent cross section σ_p^{SD} for elastic scattering. The form factors of [17] have been used for all odd-A nuclei, with the spin values of [18] used for ^{19}F; for ^{35}Cl and ^{37}Cl, the spin values are from [19], while for ^{13}C they were estimated using the odd group approximation. The Stage 2 result is seen to nearly equal the revised Stage 1 result with its revised minimum of $\sigma_p = 9.2 \times 10^{-3}$ pb at 35 GeV/c^2, despite half the exposure.

The above representation neglects the non-negligible spin contribution of the neutron sector in ^{19}F, which is captured in a model-independent SD formulation [19] with $\sigma_{\text{SD}} \sim [a_p \langle S_p \rangle + a_n \langle S_n \rangle]^2$, where $a_{p,n}$ are the WIMP-proton, neutron coupling strengths, and $\langle S_{p,n} \rangle$ are the expectation values of the proton (neutron) group spins. In this representation, experiments define a band (single nuclei targets) or an ellipse (multinuclei target), with the allowed area defined by the intersection of the most sensitive results in a_p, a_n. At $M_W = 50$ GeV/c^2, combined with neutron-sensitive XENON10 [20], the allowed area reduction is better than 2/3 compared with Ref. [1]; masses above or below this choice yield slightly increased limits for most experiments. More relevant would, however, be the model-independent results for $M_W \sim 10$ GeV/c^2, unavailable for the majority of experiments.

The impact of the results in the SI sector is shown in Fig. 4 in comparison with results from other leading search efforts [12,13,20–30], again calculated with the standard isothermal halo and WIMP elastic scattering rate of Ref. [17], using the Feldman-Cousins approach, a Helm nuclear form factor, and η'. Again, the Stage 2 contour is nearly equal to the revised Stage 1 contour with its contour minimum of 7.6×10^{-6} pb at 35 GeV/c^2. Owing to the low recoil energy threshold, both results enter the possible light mass WIMP region recently suggested by CoGeNT [30] and CRESST-II [28].

A straightforward combination of the two results using the Feldman-Cousins approach, based on 11 candidates with an assumed background 1 σ(syst) below the expected total background, yields the "merged" contours indicated in Figs. 3 and 4; in the SI case, the contour minimum drops to 4.7×10^{-6} pb and the result is in tension with the recent reports of CoGeNT [30], DAMA/LIBRA [29], and CRESST [28] regarding light mass WIMPS, using a significantly different technique with different systematics than the XENON [31] and CDMS [32] experiments. For the case of SD interactions, the contour minimum drops to 5.7×10^{-3} pb, constituting the most restrictive direct search limit on SD WIMP-proton scattering for $M_W \leq 60$ GeV/c^2 to date, and beginning to complement the more sensitive results obtained by indirect detection measurements.
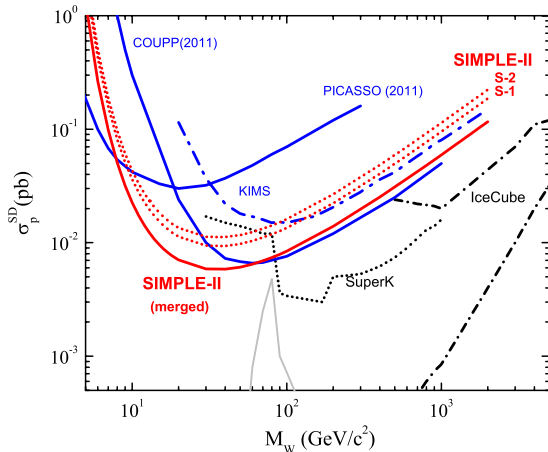

FIG. 3 (color online). Various spin-dependent WIMP-proton exclusion contours for Phase II, together with the leading direct [11–13] and indirect SuperK [14] and IceCube [15] search results; shown are the Stage 2 result, the reanalyzed Stage 1 result, and a merging of the two. The region outlined in grey is favored by cMSSM [34].
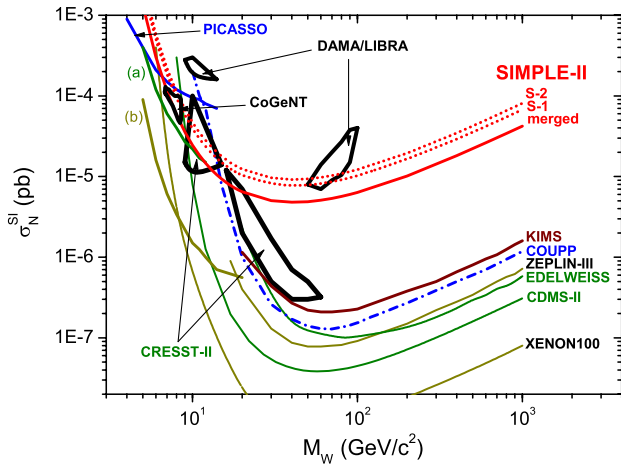
FIG. 4 (color online). Various spin-independent contours for Phase II, together with those of the leading [12,13,20–27] spin-independent search results; shown are the Stage 2 result, the reanalyzed Stage 1 result, and a merging of the two. The partial contours (a) and (b) are taken from [21,24], respectively. The closed areas identified as either CRESST-II [28], DAMA/LIBRA [29], or CoGeNT [30] represent the regions in which possible light mass WIMPS have been, respectively, reported.

The improved restrictions of the revised Stage 1 contour are a direct result of the more detailed signal analysis, improved radioassays of the shielding materials, and the revised nucleation efficiency in the analysis: Stage 2, with the additional benefit of its improved neutron shielding, provides an almost identical sensitivity with half the Stage 1 exposure. While the merging may be questioned, the results are sufficient motivation for a larger exposure measurement with further neutron background reduction, and variation of the SDD operating temperature or pressure to provide a lower recoil energy threshold, toward clarifying the situation. Variation of the refrigerant between C_3F_8, C_4F_8, CF_3I, or one of the other SDDs developed by SIMPLE in recent years [2] allows a variation of detector sensitivities between SI and SD sectors [33]. An energy spectrum can, in principle, be obtained, should candidate events be identified, by either a temperature or pressure ramping of the SDDs.

The suggested improvements in this measurement, however, also require a significantly increased active target mass in order to be competitive, for which the fabrication requirements of the current SDDs become unmanageable: a new device, originally prototyped in 2000 [7] and reprototyped in 2010, based on a large superheated freon droplet contained within a gel-sheathed vessel (effectively a bubble chamber), is currently completing development; it will permit a factor of 25 increase in the active mass with reduced space requirements. An additional all-around 60 cm of purified water shielding increases the neutron suppression by more than 10^3, giving the possibility to achieve exposures of 10^2 kgd in a few weeks.

*criodets@cii.fc.ul.pt
[1] M. Felizardo et al., Phys. Rev. Lett. **105**, 211301 (2010).
[2] T. Morlat, D. Limagne, G. Waysand, and J. I. Collar, Nucl. Instrum. Methods Phys. Res., Sect. A **560**, 339 (2006).
[3] T. Morlat, D. Limagne, G. Waysand, and J. I. Collar, Astropart. Phys. **30**, 159 (2008).
[4] T. Morlat, Ph.D. thesis, Univ. Paris 7, 2004 (unpublished).
[5] F. Seitz, Phys. Fluids **1**, 2 (1958).
[6] M. Felizardo, R. C. Martins, A. R. Ramos, T. Morlat, T. A. Girard, F. Giuliani, and J. G. Marques, Nucl. Instrum. Methods Phys. Res., Sect. A **589**, 72 (2008).
[7] J. Puibasset, Ph.D. thesis, Univ. Paris 7, 2000 (unpublished).
[8] Y. C. Lo and R. E. Apfel, Phys. Rev. A **38**, 5260 (1988).
[9] M. Barnabé-Heider et al., Nucl. Instrum. Methods Phys. Res., Sect. A **555**, 184 (2005).
[10] F. Giuliani, C. Oliveira, J. I. Collar, T. A Girard, T. Morlat, D. Limagne, J. G. Marques, A. R. Ramos, and G. Waysand, Nucl. Instrum. Methods Phys. Res., Sect. A **526**, 348 (2004).
[11] V. Zacek, Talk at TAUP-2011 Workshop, Munich, Germany, Sept. 5–9, 2011 (unpublished).
[12] W. H. Lippincott, Talk at TAUP-2011 Workshop, Munich, Germany, Sept. 5–9, 2011 (unpublished).
[13] S. K. Kim, Talk at TAUP-2011 Workshop, Munich, Germany, Sept. 5–9, 2011 (unpublished).
[14] S. Desai et al., Phys. Rev. D **70**, 083523 (2004).
[15] R. Abbasi et al., Phys. Rev. Lett. **102**, 201302 (2009).
[16] G. J. Feldman and R. D. Cousins, Phys. Rev. D **57**, 3873 (1998).
[17] J. D. Lewin and P. F. Smith, Astropart. Phys. **6**, 87(1996).
[18] A. F. Pacheco and D. Strottman, Phys. Rev. D **40**, 2131 (1989).
[19] F. Giuliani and T. A. Girard, Phys. Rev. D **71**, 123503 (2005).
[20] J. Angle et al., Phys. Rev. Lett. **100**, 021303 (2008).
[21] J. Angle et al., Phys. Rev. Lett. **107**, 051301 (2011).
[22] E. Aprile et al., Phys. Rev. Lett. **107**, 131302 (2011).
[23] Z. Ahmed et al., Science **327**, 1619 (2010).
[24] Z. Ahmed et al., Phys. Rev. Lett. **106**, 131302 (2011).

[25] V. N. Lebedenko *et al.*, Phys. Rev. D **80**, 052010 (2009).
[26] E. Armengaud *et al.*, Phys. Lett. B **687**, 294 (2010).
[27] S. Archambault *et al.*, arXiv:1202.1240v1 [Phys. Lett. B (to be published)].
[28] G. Angloher *et al.*, arXiv:1109.0702v1.
[29] C. Savage, G. Gelmini, P. Gondolo, and K. Freese, J. Cosmol. Astropart. Phys. 04 (2009) 010.
[30] C. E. Aalseth *et al.*, Phys. Rev. Lett. **106**, 131301 (2011).
[31] J. I. Collar, arXiv:1106.0653v1.
[32] J. I. Collar, arXiv:1103.3481v1.
[33] G. Bertone, D. G. Cerdeño, J. I. Collar, and B. Odom, Phys. Rev. Lett. **99**, 151301 (2007).
[34] L. Roszkowski, R. Ruiz de Austri, and R. Trotta, J. High Energy Phys. 07 (2007) 075.